MODELING AND IDENTIFICATION OF HELICOPTER EDUCATIONAL MODEL – METHODOLOGY PROPOSAL

Tomáš TKÁČIK, Anna JADLOVSKÁ
Department of Cybernetics and Artificial Intelligence, Faculty of Electrical Engineering and Informatics,
Technical University of Košice, Letná 9, 042 00 Košice, tel. 055/602 4214, E-mail: tomas.tkacik@tuke.sk

ABSTRACT

This article deals with the design of a generalized methodology for the identification of nonlinear dynamic systems using a combination of analytical and experimental identification methods. The proposed methodology is divided into modules that can be repeated if necessary. Verification of the methodology is presented on the modified helicopter educational model CE 150 from Humusoft company. A mathematical model of the system with both rotors approximated by a black-box nonlinear model is presented. The proposed experiments for obtaining experimental data are described in detail and are used in the estimation of model parameters. The gray-box model is validated in a control structure with a control law optimized for microcontrollers. Indirect validation of the gray-box model with the real helicopter educational model points to good approximation properties of the gray-box model and its potential for further use in the identification and control using artificial intelligence methods.

Keywords: *Nonlinear Dynamical Systems, Identification Methodology, Parameter Estimation, Gray-box Model, CE150 Helicopter Educational Model, Digital Control.*

1. INTRODUCTION

The helicopter educational model designed by Humusoft company is an unstable system with two degrees of freedom. The educational model is mainly used for educational and research activities in the system identification and design of control algorithms. The helicopter educational model can partially rotate in elevation and azimuth angle while being controlled by two rotors. The presence of strong cross-coupling between elevation and azimuth is challenging mainly in the system identification. The third control element (balancing weight) can be used in the robustness verification of the designed control algorithms. The principles and experiences from the educational model can be used in the field of unmanned aerial vehicles.

In the research, the CE 150 helicopter educational model has been used in many system identification and control design applications. In [1–3], authors derived a mathematical model of the system in the form of differential equations using the Euler-Lagrange method. The mathematical model derived in the educational tutorial [4] was used in [5–7] including the parameters. Additionally, in [3, 8] the parameters of the mathematical model were estimated using genetic algorithms. A set of linear black-box models was identified in [9] at different operational points to capture the nonlinear properties of the system. In [1], the authors used a neural network to approximate the dynamics of the system. From control design perspective, input-output [5, 7, 10], state-space [5], robust [2, 6, 10–13], self-tuning [12], predictive [14] and fuzzy [6, 8, 15] control algorithms were used to control the helicopter educational model. In [1], the authors used feedback linearization to compensate for nonlinearities, and in [16] the model-free control algorithm design with neural network discriminator was proposed. In [15], the authors modified the educational model of the helicopter from Humusoft by replacing the lab card with Arduino Mega and by adding an IMU (inertial measurement unit) sensor to measure angular speed of elevation and azimuth. In addition to the model from Humusoft, the authors used helicopter model from Quanser [2, 16], or designed and built their own model [1, 3].

In the research group the Center of Modern Control Techniques and Industrial Informatics (CMCT&II) at the Department of Cybernetics and Artificial Intelligence (DCAI) at the Faculty of Electrical Engineering and Informatics (FEEI) at the Technical University (TU) of Košice, the authors of this article are part of, the helicopter educational model was used in the research and educational activities. In the research, linear structures using input-output regression models ARX and ARMAX [17] and linear state models [17, 18] were used in the identification of the helicopter educational model. Similarly, non-linear model structures were also used, e.g. single step predictors based on neural networks [19] or analytical model from the educational tutorial [4]. In [17], the experimental identification methodology is presented, including model validation using the analysis of model residuals in *Matlab/Simulink* environment. Identified models were subsequently used to design control algorithms, e.g. input-output control synthesized using the pole placement method [17], state-space control with integrator [17, 18], model-predictive control [19], and neural network model-predictive control [19]. Various control structures have been used, including feed-forward nonlinearity compensation with polynomial approximation [17] and discrete Kalman state estimator [19].

In this article, a complex methodology for the nonlinear system modeling and identification is proposed, which is verified in the case study realized on the helicopter educational model. Modifications to the mathematical model of the CE 150 helicopter educational model are presented in the analytical identification. Parameters of the mathematical model are estimated using experimental identification. Newly designed experiments with additional sensors are presented, as input-out data used previously is deemed insufficient. The selected model structure requires the choice of more advanced methods of nonlinear parameter estimation,where the combination of genetic algorithms and surrogate optimization is selected. An indirect validation of the

identified model is performed in a control structure using the polynomial control algorithm with instantaneous linearization, which has been implemented into STM32 microcontroller. The resulting model is considered as the digital twin of the helicopter educational model, because it closely matches the dynamics of the real system. The potential of the digital twin of the helicopter educational model lies in the creation of intelligent neural network-based models.

In section 2, the proposed methodology for the identification of unstable nonlinear MIMO dynamical systems is presented, which unifies analytical and experimental identification methods. The verification of the proposed methodology is presented in section 3 as part of the case study focused on the identification of the helicopter educational model. The case study includes the derivation of the mathematical model of the nonlinear dynamical system, a detailed description of the designed experiments, estimation of the model parameters, and validation of the model in a control structure. The obtained results are evaluated in conclusions section with the main contributions pointed out.

2. DESIGN OF METHODOLOGY FOR MODELING AND IDENTIFICATION OF NONLINEAR DYNAMICAL SYSTEMS

The proposed generalized methodology for modeling and identification of nonlinear dynamic systems (NDS) is shown in Fig. 1. The methodology is designed to combine the principles of analytical and experimental identification. The resulting model thus belongs to the group of gray-box models that use a combination of physics insight and data-driven methods. The reviewed literature [20–23] mentions the advantages of combining analytical and experimental identification but lacks a description of the overall methodology combining both principles. One of the contributions of this article is the proposal of a unifying methodology.

The proposed methodology consists of 4 modules: *Analysis*, *Data collection*, *Parameter estimation*, and *Model validation*. The **Analysis module** uses the principles of analytical identification to create a mathematical model of the identified system. It is divided into 4 submodules:
A1. *System decomposition* - the purpose of decomposition is to divide the identified system into subsystems to make it easier to derive mathematical model,
A2. *Subsystem modeling* - a mathematical model of each subsystem is derived using natural laws, such as balance equations,
A3. *Model substitution* - in case the mathematical model of the subsystem is complex, it is advisable to choose its approximation, e.g. substitution with a black-box model,
A4. *Mathematical model formulation* - derived models of individual subsystems are combined to obtain a mathematical model of the identified system.

The **Data collection module** is focused on obtaining and preparing experimental data that capture the dynamics of the identified system. It consists of 3 submodules:
C1. *Experiment design* - an experiment on the identified system is designed and prepared,
C2. *Data recording* - data from the experiment is recorded with the selected sampling period T_s,
C3. *Data processing* - recorded data is further processed in order to remove noise, normalize data, etc.

The **Parameter estimation module** is used to estimate model parameters in the selected structure from the *Analysis module*. The module consists of three submodules:
E1. *Optimization method selection* - based on the chosen structure of the mathematical model, a suitable method for parameter estimation is selected,
E2. *Design of criteria function* - the criteria function design must take into account the weighting of system outputs, parameter sensitivity, and data quality,
E3. *Parameter estimation* - the selected optimization method and criterion function are applied to obtain the parameter values of the mathematical model.

The **Model validation module** verifies the approximation capabilities of the gray-box model. In the proposed methodology, the identified model is validated in the control structure with the aim of generalizing the methodology for unstable systems. It consists of two submodules:
V1. *Control law design* - a stabilizing control law is designed based on the identified gray-box model,
V2. *Validation in control structure* - the designed control algorithm is applied to the mathematical model and the identified system, while the inputs and outputs are compared.

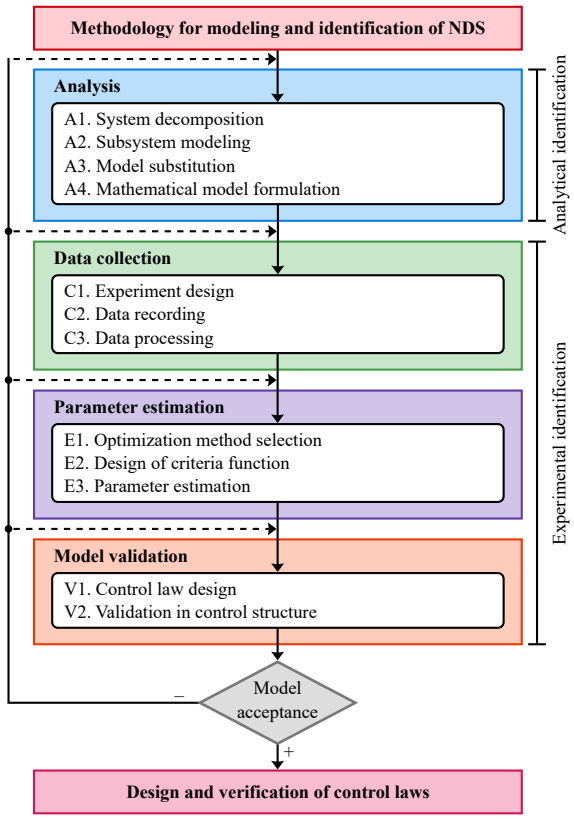

Fig. 1 Methodology for modeling and identification of nonlinear dynamic systems (NDS).

In case the validation is unsatisfactory, individual steps of the proposed methodology can be repeated in order to obtain a more suitable model. The validated gray-box model can be used in analysis, control law design using classical and intelligent methods, or diagnostics. In the next section, the proposed NDS identification methodology is verified on the helicopter educational model made by Humusoft company.

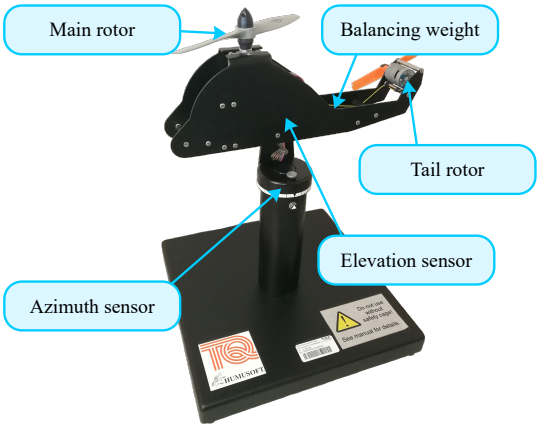

Fig. 2 CE 150 Helicopter Educational Model.

3. VERIFICATION OF PROPOSED METHODOLOGY ON THE MODIFIED HELICOPTER EDUCATIONAL MODEL - CASE STUDY

In this section, the proposed methodology is verified by the case study of the modified helicopter educational model identification in the structure of the gray-box model. The helicopter educational model is based on the CE 150 helicopter model from Humusoft company shown in Fig. 2. The proposed modification replaces the MF-624 laboratory card with an STM32G071-based development board with the USB-UART communication interface. This modification ensures compatibility with modern computers. A communication protocol is proposed that sends binary data bidirectionally via the USB-UART serial interface. This enables interactive integration of the helicopter educational model in the Simulink simulation environment, similarly to the hardware in a loop simulation paradigm.

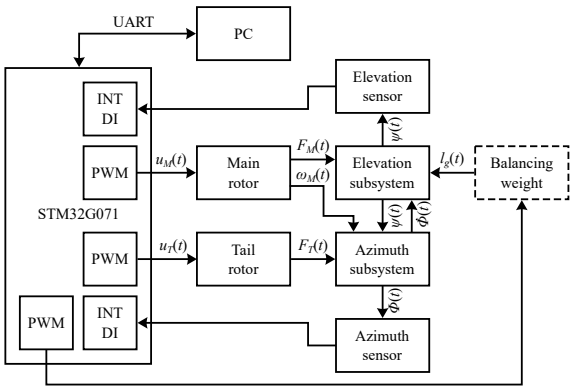

Fig. 3 Decomposition of CE 150 Helicopter into subsystems.

3.1. Mathematical modeling

The modified helicopter educational model is identified using the methodology presented in section 2. Within the **Analysis module**, the *Model decomposition* (A1) is performed first, as shown in Fig. 3. From the listed subsystems, only the main and auxiliary rotor subsystems and the elevation and azimuth subsystems are considered. The elevation and azimuth sensors use an incremental encoder for position sensing, the dynamics of which are significantly faster compared to other subsystems. Therefore, both sensors are modeled statically. The balancing weight subsystem is also not considered, as our intent is to use it as a fault signal in the control algorithm verification.

Selected subsystems (main and tail rotor subsystems, elevation and azimuth subsystems) are modeled separately in the *Subsystem modeling* (A2) submodule. Both rotors of the educational model consist of a DC motor to which the propeller is directly attached (without a gearbox). A DC motor can be modeled using Kirchhoff's second law

$$L\frac{di(t)}{dt} + Ri(t) + K_e\omega(t) = u(t) \tag{1}$$

where L [H] is coil inductance, $i(t)$ [A] is a coil current, R [Ω] is coil resistance, K_e [V.s.rad^{-1}] is motor electromotive constant, $\omega(t)$ [rad.s^{-1}] is motor angular velocity, $u(t)$ [V] is applied voltage, and the balance equation of rotary motion

$$J\dot{\omega}(t) + b\omega(t) = K_t i(t) \tag{2}$$

where J [kg.m^2] is motor inertia, b [N.m.s] is friction constant K_t [N.m.A^{-1}] is motor torque constant (numerically $K_t = K_e$). The rotor thrust force $F_a(t)$ [N] depends on the angular velocity $\omega(t)$ of the rotor and can be modeled using static gain as

$$F_a(t) = \rho A K_a \omega^2(t) \tag{3}$$

where $F_a(t)$ is trust force produced, ρ [kg.m^{-3}] is air density, A [m^2] is propeller area cross-section, K_a [m^2.rad^{-2}] is coefficient of air speed dependence on motor angular velocity $\omega(t)$ [24]. Such a rotor model contains many parameters that must be identified. Also, the model is based on several assumptions and simplifications (e.g. it does not consider thrust reduction by air flow being obstructed by the helicopter's body). For the stated reasons, a *Model substitution* (A3) was opted for. In [25], the DC motor is modelled using a black-box model (first-order transfer function). Such a simplification was sufficient due to the narrow speed range of the fan. Since a wider speed range is expected in the case of the helicopter's rotors, the damping is modeled using polynomials due to their excellent approximation properties. The nonlinear black-box model of the main rotor is proposed as

$$\dot{\omega}_M(t) + \underbrace{\sum_{i=0}^{2} p_{b_{M(i)}}\omega_M^i(t)}_{P_{b_M}(\omega_M(t))}\omega_M(t) = K_M u_M(t) \tag{4}$$

where $\omega_M(t)$ [rad.s^{-1}] is main rotor speed, $p_{b_{M(i)}}$ is i-th coefficient of a 2nd degree polynomial $P_{b_M}(\omega_M(t))$ [s^{-1}] approximating friction, K_M [rad.s^{-2}.V^{-1}] is main rotor constant, and $u_M(t)$ [V] is main rotor input voltage.

Similarly, the nonlinear black-box model of the tail rotor is proposed as

$$\dot{\omega}_T(t) + \underbrace{\sum_{i=0}^{2} p_{b_{T(i)}}\omega_T^i(t)}_{P_{b_T}(\omega_T(t))}\omega_T(t) = K_T u_T(t) \tag{5}$$

where $\omega_T(t)$ [rad.s^{-1}] is tail rotor speed, $p_{b_T(i)}$ is i-th coefficient of a 2nd degree polynomial $P_{b_T}(\omega_T(t))$ [s^{-1}] approximating friction, K_T [rad.s^{-2}.V^{-1}] is tail rotor constant, and $u_T(t)$ [V] is tail rotor input voltage.

The thrust force $F(t)$ [N] generated by a spinning propeller can be derived analytically. However, the analytical model is based on many simplifications and does not take physical dimensions into account. Therefore, it is better to model the rotor's thrust force using a nonlinear black-box model. The main rotor thrust force $F_M(t)$ [N] is therefore modeled as

$$F_M(t) = \underbrace{\sum_{i=0}^{4} p_{F_M(i)} \omega_M^i(t)}_{P_{F_M}(\omega_M(t))} \tag{6}$$

where $p_{F_M(i)}$ is i-th coefficient of a 4th degree polynomial $P_{F_M}(\omega_M(t))$ [N] approximating dependence of main rotor thrust force $F_M(t)$ on main rotor speed $\omega_M(t)$.

The tail rotor thrust force $F_T(t)$ [N] is modeled as

$$F_T(t) = \underbrace{\sum_{i=0}^{4} p_{F_T(i)} \omega_T^i(t)}_{P_{F_T}(\omega_T(t))} \tag{7}$$

where $p_{F_T(i)}$ is i-th coefficient of a 4th degree polynomial $P_{F_T}(\omega_T(t))$ [N] approximating dependence of tail rotor thrust force $F_T(t)$ on tail rotor speed $\omega_T(t)$.

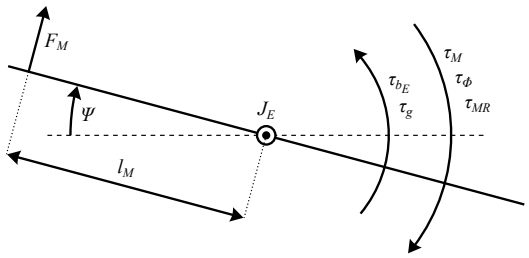

Fig. 4 Elevation subsystem schematic.

The model of the elevation subsystem (see Fig. 4) can be derived by constructing the balance equation of the rotary motion, by considering the moment of influence of the main rotor $\tau_M(t)$ [N.m], the centrifugal moment due to rotation in azimuth $\tau_\Phi(t)$ [N.m], the gravitational torque τ_g [N.m], the moment of friction (Coulomb and viscous friction) $\tau_{b_E}(t)$ [N.m], and the moment of gyroscopic effect $\tau_{MR}(t)$ [N.m]. The model of the elevation subsystem is formulated as

$$\begin{aligned} \underbrace{J_E\ddot{\Psi}(t)}_{\tau_E(t)} = \underbrace{l_M F_M(t)}_{\tau_M(t)} + \underbrace{\frac{\tau_{g_E}}{2g}\dot{\Phi}^2(t)\sin(2\Psi(t))}_{\tau_\Phi(t)} - \\ - \underbrace{\tau_{g_E}\cos(\Psi(t))}_{\tau_g(t)} - \underbrace{(b_{v_E}\dot{\Psi}(t) + b_{c_E}\,\mathrm{sgn}(\dot{\Psi}(t)))}_{\tau_{b_E}(t)} + \\ + \underbrace{K_E\dot{\Phi}(t)\omega_M(t)\sin(\Psi(t))}_{\tau_{MR}(t)} \end{aligned} \tag{8}$$

where J_E [kg.m^2] is moment of inertia of the elevation subsystem, $\Psi(t)$ [rad] is elevation angle, $\tau_E(t)$ [N.m] is final torque applied to elevation subsystem, l_m [m] is distance between main rotor and elevation axis, τ_{g_E} [N.m] is base gravitational torque, g [m.s^{-2}] is gravitational acceleration, $\Phi(t)$ [rad] is azimuth angle, b_{v_E} [N.m.s] is coefficient of viscous friction, b_{c_E} [N.m] is coefficient of Coulomb friction, and K_E [kg.m^2.rad^{-1}] is coefficient of gyroscopic effect.

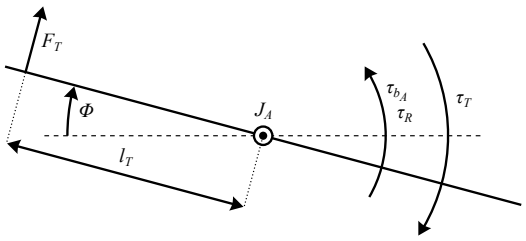

Fig. 5 Azimuth subsystem schematic.

Derivation of the azimuth subsystem (see Fig. 5) model requires the construction of a balance equation. Considering the moment of the tail rotor influenced by the elevation angle $\tau_T(t)$ [N.m], the reactive moment of the main rotor $\tau_{TR}(t)$ [N.m], and the moment of friction (Coulomb and viscous friction) $\tau_{b_A}(t)$ [N.m], the azimuth subsystem model is formulated as

$$\begin{aligned} \underbrace{J_A\cos(\Psi(t))\ddot{\Phi}(t)}_{\tau_A(t)} = \underbrace{l_T F_T(t)\cos(\Psi(t))}_{\tau_T(t)} - \\ - \underbrace{K_A\omega_M(t)\cos(\Psi(t))}_{\tau_{TR}(t)} - \underbrace{(b_{v_A}\dot{\Phi}(t) + b_{c_A}\,\mathrm{sgn}(\dot{\Phi}(t)))}_{\tau_{b_A}(t)} \end{aligned} \tag{9}$$

where J_A [kg.m^2] is moment of inertia of the azimuth subsystem, l_T [m] is distance between the tail rotor and azimuth axis, K_A [N.m.s] is coefficient of reactive moment of the main rotor, b_{v_A} [N.m.s] is coefficient of viscous friction, and b_{c_A} [N.m] is coefficient of Coulomb friction. Models of the elevation (8) and azimuth (9) subsystem were adopted from the educational tutorial [4].

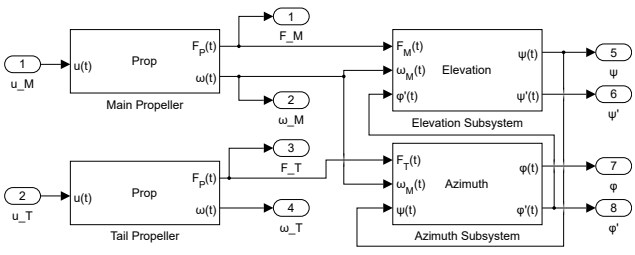

Fig. 6 Gray-box model of the Helicopter Educational Model in Simulink.

The final mathematical model is formulated by combining models of all subsystems represented by equations (4, 5, 8, 9) in the *Model formulation* (A4) submodule of the proposed methodology. In this submodule, the obtained mathematical model is implemented into the Simulink simulation environment, as shown in Fig. 6. The model implementation in the Simulink allows for convenient parameter estimation and control algorithm verification later on.

The obtained mathematical model of the helicopter educational model formulated in this way defines a structure, whose parameter values are not known. Therefore, it is necessary to proceed with modules based on the experimental identification methods in the presented methodology.

3.2. Capturing system dynamics

The unknown parameter values of the mathematical model are to be estimated from the experimental data prepared in the **Data collection module**.

For reliable parameter estimation, the *Experiment design* (C1) is essential, as experiments capture the dynamics of the identified system.

The design of the experiments can utilize the already performed system decomposition, as the design of experiments and the subsequent parameter estimation done individually for each subsystem lowers the overall computational complexity. To identify the helicopter educational model, nine experiments are proposed.

In the *1st experiment*, a rectangular signal $u_M(t)$ with random amplitude and period is applied to the main rotor. The rotor thrust force $F_M(t)$ and the angular velocity ω_M are recorded using a load cell and photogate respectively.

The *2nd experiment* is similar to the *1st experiment* as the scenario has been repeated for the tail rotor to capture its dynamics.

The *3rd experiment* is focused on the estimation of base gravitational torque τ_{g_E} by balancing the elevation subsystem with additional counterweights added to the tail of the helicopter body. After settling and reaching the balance, the elevation angle Ψ and counterweight weight m_Δ are recorded. The azimuth subsystem is locked.

In the *4th experiment*, the autonomous elevation subsystem is turned by 90°to change the direction of gravitational force action. Disturbing the elevation subsystem from its equilibrium state causes self-oscillations to occur, that are recorded. The azimuth subsystem is locked.

The *5th experiment* is performed with the azimuth subsystem locked. Various input voltages $u_M(t)$ are applied to the main rotor of the helicopter, while the elevation angle $\Psi(t)$ does not exceed the center of the operational range $\Psi < 0$. This experiment captures the dynamics of the autonomous elevation subsystem in its stable region.

In the *6th experiment*, the autonomous azimuth subsystem is rotated by 90°. By disturbing the azimuth subsystem from its equilibrium, autonomous oscillations are achieved. The elevation subsystem is locked.

The *7th experiment* requires that the elevation subsystem is locked, and a simple rule-based azimuth subsystem control algorithm is designed. The designed control algorithm ensures stable oscillations of the azimuth subsystem within its operational limits.

During the *8th experiment*, the elevation subsystem is locked, and the main rotor input signal $u_M(t)$ is varied. For each value, a corresponding tail rotor input $u_T(t)$ is experimentally searched that compensates for the reactive moment of the main rotor on the azimuth subsystem.

In the *9th experiment*, the input signal $u_M(t)$ of the main rotor is varied while the azimuth subsystem is rotated manually around its axis. This experiment captures the effect of the rotation of the azimuth subsystem on the elevation subsystem.

The *Data recording* (C2) submodule is used to record data from the proposed experiments with a sampling period of $T_s = 0.01$ [s] (100 [Hz]). The choice of the sampling period is based on the educational manual [4]. In case the sampling period is too short, the data can be resampled in the data processing module later. The only exception to the selected sampling period is *1st* and *2nd experiment*, in which the HX711 module is used to measure thrust with a load cell at a sampling frequency of 10 [Hz] and a digital oscilloscope for measuring angular velocity photogate pulses running at a sampling frequency of 10 [MHz].

In the *Data processing* (C3) submodule, it is necessary to process the data from *1st* and *2nd experiment*. The pulses from the photogate are converted to the angular velocity of individual rotors while considering the number of propeller blades. An additional STM32-based development board is used to read the data from the load cell. A single digital pulse is used to synchronize the time between the oscilloscope and the development boards. The data measured from *8th experiment* also requires preprocessing, where azimuth velocity is calculated using a difference of the azimuth angle that is later smoothed using the median filter. Preprocessing data from other experiments requires only trimming. This is due to the behavior of the identified system at the beginning of each experiment that could not be fully explained by the model. Data processed in this way can be used to estimate unknown parameter values.

3.3. Estimation of model parameters

In the **Parameter estimation module**, the estimation of unknown parameter values of the mathematical model $\boldsymbol{\varphi} = [p_{b_M0},\ p_{b_M1},\ p_{b_M2},\ K_M,\ p_{b_T0},\ p_{b_T1},\ p_{b_T2},\ K_T,\ p_{F_M0},\ p_{F_M1},\ F_{b_M2},\ F_{b_M3},\ F_{b_M4},\ p_{F_T0},\ p_{F_T1},\ F_{b_T2},\ F_{b_T3},\ F_{b_T4},\ J_E,\ \tau_{g_E},\ b_{v_E},\ b_{c_E},\ K_E,\ J_A,\ K_A,\ b_{v_A},\ b_{c_A}]$ is dealt with. As part of the *Optimization method selection* (E1) submodule, suitable optimization methods are selected. The following three optimization methods are selected: nonlinear least squares method, surrogate optimization, and genetic algorithms. Surrogate optimization and genetic algorithms are used for the initial estimation of unknown parameter values with consequential fine-tuning using the nonlinear least squares method. The surrogate optimization method is suitable for quick estimation of a smaller number of parameters. With a larger number of parameters to be estimated, genetic algorithms are preferred as they allow to search the entire solution space.

The estimation of unknown parameter values $\boldsymbol{\varphi}$ is performed for subsystems separately. The experiments are designed in a way that the data can be used for the estimation of the fewest parameters per experiment, which simplifies the *Design of criteria function* (E2). A generic quadratic criterion function is selected in the form

$$V(\boldsymbol{\varphi}) = \sum_{k=1}^{N} \boldsymbol{\varepsilon}^T(k,\boldsymbol{\varphi}) \boldsymbol{Q_V} \boldsymbol{\varepsilon}(k,\boldsymbol{\varphi}) \tag{10}$$

where $\boldsymbol{\varepsilon}(k,\boldsymbol{\varphi})$ is prediction error vector and $\boldsymbol{Q_V}$ is the weighting matrix. The weighting matrix $\boldsymbol{Q_V}$ can be omitted in systems with a single output, as it has no effect on the parameter estimation. Parameter estimation of the helicopter educational model requires a diagonal positive definite weighting matrix $\boldsymbol{Q_V}$ for the first two experiments to scale the values of the angular velocity of the rotors and the

thrust of the rotors. Otherwise, the weighting matrix $\boldsymbol{Q_V}$ is omitted as the output prediction error is scalar.

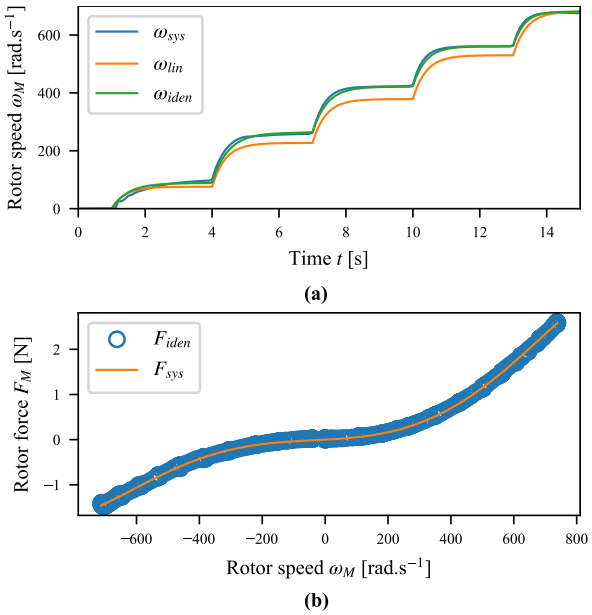

Fig. 7 Main rotor subsystem parameter estimation; **(a)** main rotor speed ω_M; **(b)** main rotor thrust F_M.

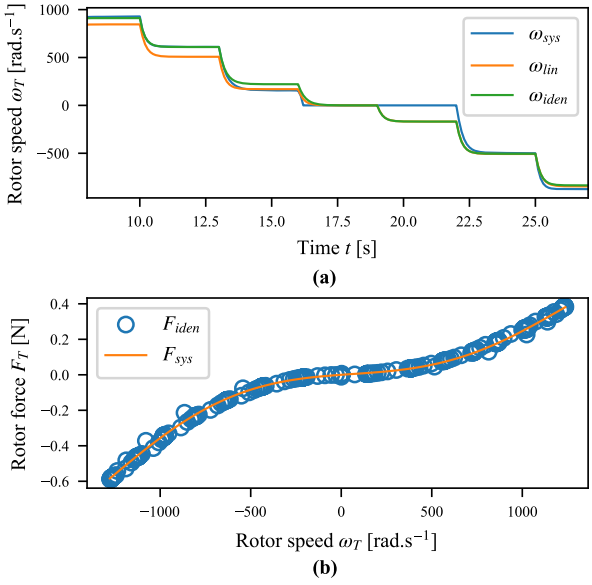

Fig. 8 Tail rotor subsystem parameter estimation; **(a)** tail rotor speed ω_M; **(b)** tail rotor thrust F_M.

The *Parameter estimation* (E3) relies on the minimization of the selected criterion function $V(\boldsymbol{\varphi})$. This results in the overall reduction of the prediction error $\boldsymbol{\varepsilon}(k,\boldsymbol{\varphi})$ thus allowing the model to approximate the dynamics of the real system. The parameters are estimated using the *Simulink Design Optimization Toolbox* in the Simulink simulation environment. The parameters of the main and tail rotor subsystems are estimated from the first two experiments, with results shown in Fig. 7 and Fig. 8 , where lower indexes *sys* and *iden* denote experimental data and output of the nonlinear model respectively. For comparison, the results are compared to the linear structure (lower index *lin*) of the rotor model described in the educational manual [4].

Fig. 10 displays the estimation of the base gravity moment τ_{g_E}. The experiment is based on the schematic of the elevation subsystem considering the counterweight shown in Fig. 9. Mathematically, it can be expressed from (8) as

$$\tau_{g_E}\cos(\Psi+\Psi_m) = l_{m_\Delta} m_\Delta g \cos(\Psi+\Psi_{m_\Delta}) \tag{11}$$

where Ψ_m and Ψ_{m_Δ} are angular deviations from elevation axis, l_{m_Δ} is distance between elevation axis and counterweight, and m_Δ is counterweight mass.

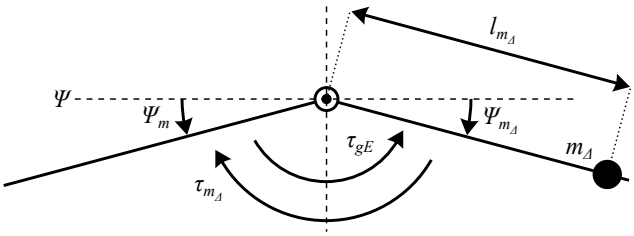

Fig. 9 Estimation of base gravitational torque τ_{g_E} - elevation subsystem schematic.

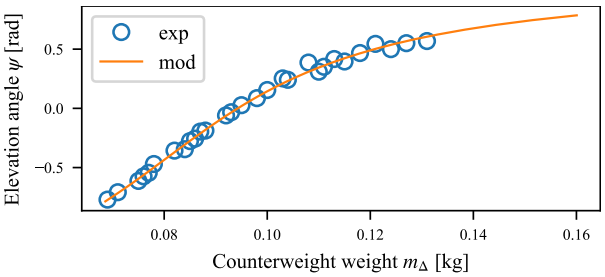

Fig. 10 Estimation of base gravitational torque τ_{g_E}.

Data from the remaining experiments is used to estimate the unknown parameter values of the elevation and azimuth subsystems. A model with estimated parameter values $\boldsymbol{\varphi}$ must be validated before it can be used in other tasks, such as control algorithm design.

3.4. Validation of the gray-box model in control structure

Since the helicopter educational model is unstable in an open-loop, **Model validation module** is performed in the control structure. This requires the *Control law design* (V1). A polynomial control algorithm with instantaneous linearization is selected. The design of a polynomial control algorithm requires a linearized and discretized model of the helicopter educational model in transfer function form. The state vector of the helicopter educational model is

$$\begin{aligned}\boldsymbol{x}(t) &= [x_1(t) \quad x_2(t) \quad x_3(t) \quad x_4(t) \quad x_5(t) \quad x_6(t)]^T = \\ &= [\omega_M(t) \quad \Psi(t) \quad \dot{\Psi}(t) \quad \omega_T(t) \quad \Phi(t) \quad \dot{\Phi}(t)]^T\end{aligned} \tag{12}$$

and the vector of inputs is

$$\boldsymbol{u}(t) = [u_M(t) \quad u_T(t)]^T \tag{13}$$

The mathematical model of the helicopter educational model can be represented by a vector function of state variables evolution in time as follows

$$\dot{\boldsymbol{x}}(t) = \boldsymbol{f_c}(t,\boldsymbol{x}(t),\boldsymbol{u}(t)) \tag{14}$$

which can be expanded to the system of nonlinear differential equations as follows

$$\begin{aligned}
\dot{x}_1(t) &= -P_{b_M}(x_1(t))x_1(t) + K_M u_M(t)\\
\dot{x}_2(t) &= x_3(t)\\
\dot{x}_3(t) &= \frac{\tau_M(x_1)+\tau_{\dot{\Phi}}(x_2,x_6)-\tau_g(x_2)-\tau_{b_E}(x_3)+\tau_{MR}(x_1,x_2,x_6)}{J_E}\\
\dot{x}_4(t) &= -P_{b_T}(x_4(t))x_4(t) + K_T u_T(t)\\
\dot{x}_5(t) &= x_6(t)\\
\dot{x}_6(t) &= \frac{\tau_T(x_2,x_4)-\tau_{TR}(x_1,x_2)-\tau_{b_A}(x_6)}{J_A}
\end{aligned} \tag{15}$$

The model (14) is linearized at the selected operating point

$$\boldsymbol{OP} = [x_{10} \quad x_{20} \quad x_{30} \quad x_{40} \quad x_{50} \quad x_{60} \quad u_{M0} \quad u_{T0}]^T \tag{16}$$

The operating point $\boldsymbol{OP}$ is calculated by solving a system of algebraic equations $\boldsymbol{f_c}(\cdot) = \boldsymbol{0}$ at selected elevation angle Ψ_0. A linearized perturbation state-space model of the system is derived by calculating the Jacobians of the state function $\boldsymbol{f_c}(\cdot)$ as

$$\boldsymbol{A} = \left.\frac{\partial \boldsymbol{f_c}(t,\boldsymbol{x}(t),\boldsymbol{u}(t))}{\partial \boldsymbol{x}(t)}\right|_{\boldsymbol{OP}}; \boldsymbol{B} = \left.\frac{\partial \boldsymbol{f_c}(t,\boldsymbol{x}(t),\boldsymbol{u}(t))}{\partial \boldsymbol{u}(t)}\right|_{\boldsymbol{OP}} \tag{17}$$

where $\boldsymbol{A}$ and $\boldsymbol{B}$ are the matrices of the linear state-space perturbation model of the system at the selected operating point $\boldsymbol{OP}$. The matrix $\boldsymbol{C}$ is defined as

$$\boldsymbol{C} = \begin{bmatrix} 0 & 1 & 0 & 0 & 0 & 0 \\ 0 & 0 & 0 & 0 & 1 & 0 \end{bmatrix} \tag{18}$$

and the matrix $\boldsymbol{D}$ is zero. The linearized state-space perturbation model is defined as

$$\begin{aligned}
\Delta\dot{\boldsymbol{x}}(t) &= \boldsymbol{A}\Delta\boldsymbol{x}(t) + \boldsymbol{B}\Delta\boldsymbol{u}(t)\\
\Delta\boldsymbol{y}(t) &= \boldsymbol{C}\Delta\boldsymbol{x}(t) + \boldsymbol{D}\Delta\boldsymbol{u}(t)
\end{aligned} \tag{19}$$

where $\Delta\boldsymbol{x}(t) = \boldsymbol{x}(t) - \boldsymbol{x_{OP}}$, $\Delta\boldsymbol{u}(t) = \boldsymbol{u}(t) - \boldsymbol{u_{OP}}$, and $\Delta\boldsymbol{y}(t) = \boldsymbol{y}(t) - \boldsymbol{y_{OP}}$. The linearized perturbation model is discretized using the *c2d* function and converted into a transfer function using the *ss2tf* function. Both functions are implemented in the *Control System Toolbox* in *Matlab*. In the following, only the transfer function of *elevation angle to main rotor input*

$$F_{\Psi/U_M}(z) = \frac{B_{el}(z)}{A_{el}(z)} = \frac{b_{el1}z^{-1} + b_{el2}z^{-2} + b_{el3}z^{-3}}{a_{el0} + a_{el1}z^{-1} + a_{el2}z^{-2} + a_{el3}z^{-3}} \tag{20}$$

and *azimuth angle to tail rotor input*

$$F_{\Phi/U_T}(z) = \frac{B_{az}(z)}{A_{az}(z)} = \frac{b_{az1}z^{-1} + b_{az2}z^{-2} + b_{az3}z^{-3}}{a_{az0} + a_{az1}z^{-1} + a_{az2}z^{-2} + a_{az3}z^{-3}} \tag{21}$$

is considered. $A_{el}(z)$ and $B_{el}(z)$ are denominator and numerator polynomials of the elevation subsystem transfer function of rank $n_{el} = 3$ and $m_{el} = 2$ respectively. Similarly, $A_{az}(z)$ and $B_{az}(z)$ are denominator and numerator polynomials of the azimuth subsystem transfer function of rank $n_{az} = 3$ and $m_{az} = 2$ respectively. Other transfer functions are ignored in the design of the control algorithm.

The transfer function of the polynomial controller for the elevation subsystem $F_{U_M/E_\Psi}(z)$ and for the azimuth subsystem $F_{U_T/E_\Phi}(z)$ must be of the same rank as the controlled subsystem. The elevation subsystem polynomial controller transfer function is defined as

$$F_{U_M/E_\Psi}(z) = \frac{Q_{el}(z)}{P_{el}(z)} = \frac{q_{el0} + q_{el1}z^{-1} + q_{el2}z^{-2} + q_{el3}z^{-3}}{1 + p_{el1}z^{-1} + p_{el2}z^{-2} + p_{el3}z^{-3}} \tag{22}$$

where $Q_{el}(z)$ and $P_{el}(z)$ are numerator and denominator polynomials of the transfer function of rank $n_{Qel} = 3$ and $n_{Pel} = 3$ respectively. A suitable method to calculated the elevation subsystem controller parameters $\boldsymbol{\varphi}_{elcl} = [q_{el0} \ \ldots \ q_{el3} \ p_{el1} \ \ldots \ p_{el3}]^T$ is the pole-placement method. The transfer function of the control structure is formulated using the elevation subsystem (20) and polynomial controller (22) transfer functions as

$$\begin{aligned}
F_{\Psi/\Psi_{ref}}(z) &= \frac{F_{\Psi/U_M}(z)F_{U_M/E_\Psi}(z)}{1 + F_{\Psi/U_M}(z)F_{U_M/E_\Psi}(z)} =\\
&= \frac{B_{el}(z)Q_{el}(z)}{A_{el}(z)P_{el}(z) + B_{el}(z)Q_{el}(z)}
\end{aligned} \tag{23}$$

The characteristic polynomial $P_{elcl}(z, \boldsymbol{\varphi}_{elcl})$ of the control structure (23) is thus defined as

$$P_{elcl}(z, \boldsymbol{\varphi}_{elcl}) = A_{el}(z)P_{el}(z) + B_{el}(z)Q_{el}(z) \tag{24}$$

whose rank is twice the system rank $n_{P_{elcl}} = 6$. To design the polynomial control algorithm using the pole-placement method, a reference characteristic polynomial $P^*_{elcl}(z)$ of rank $n_{P^*_{elcl}} = 6$ is constructed based on the experimentally selected poles $(z_1^*, z_2^*, \ldots, z_6^*)$ of the control structure as

$$P^*_{elcl}(z) = \prod_{i=1}^{6}(z - z_i^*) \tag{25}$$

Coefficients of the elevation subsystem controller $\boldsymbol{\varphi}_{elcl}$ are calculated by comparing the coefficients of the same exponent of the control structure characteristic polynomial (24) with the coefficients of the reference characteristic polynomial (25) as follows

$$A_{el}(z)P_{el}(z) + B_{el}(z)Q_{el}(z) = \prod_{i=1}^{6}(z - z_i^*) \tag{26}$$

which yields system of 7 algebraic equations. Finally, the feedback control law $u_{Mfb}(k)$ is formulated as

$$\begin{aligned}
u_{Mfb}(k) = &\sum_{i=0}^{3}(q_{el\,i}(k-i)e_\Psi(k-i)) -\\
&- \sum_{i=1}^{3}(p_{el\,i}(k-i)u_M(k-i))
\end{aligned} \tag{27}$$

To compensate for the nonlinearities of the elevation subsystem, a feedforward controller is proposed. The amplitude of the input signal is set by the operating point $\boldsymbol{OP}$ to be equal to $u_{Mf0} = u_{M0}$. The elevation control algorithm at the selected operating point $\boldsymbol{OP}$ is defined as

$$u_M(k) = u_{Mfb}(k) + u_{Mf0} \tag{28}$$

The design of feedback u_{Mfb} and feedforward u_{Mff} control algorithms is repeated for operating points with different elevation angles Ψ across the whole operational range of the elevation subsystem. The feedforward control algorithm action is approximated by 2nd-degree polynomial $u_{Mff}(\Psi) = P_{u_{Mff}}(\Psi)$. A set of feedback control algorithms is designed for the elevation subsystem at each operating point. To avoid sudden spikes in the control input when the system transitions from one operating point to another, coefficients of the control algorithm for the elevation subsystem are approximated with 3rd-degree polynomials $q_{el0}(\Psi) = P_{q_{el0}}(\Psi)$. Such modification allows to store controller parameters in the memory of constant size defined by the polynomial degree and system rank while providing reduced computational needs compared to the instantaneous linearization approach. This makes it perfect for direct implementation in the microcontroller firmware. A separate control algorithm is designed for the azimuth subsystem in a similar way $u_T(k) = u_{Tfb}(k) + u_{Tff}(\Psi)$, whose coefficients also depend on the elevation angle Ψ. The proposed control structure in depicted in Fig. 11.

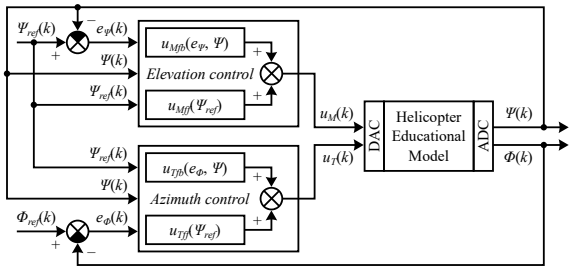

Fig. 11 The control structure with feedback and feedforward control algorithms for elevation and azimuth subsystems.

The designed control structure is used in *Validation in control structure* (V2) submodule to assert the validity of the gray-box model with identified parameters. Indirect model validation is performed by comparing the inputs and outputs of the gray-box model implemented in the simulation environment with the real helicopter educational model. The control structure used in the gray-box model validation is shown in Fig. 12.

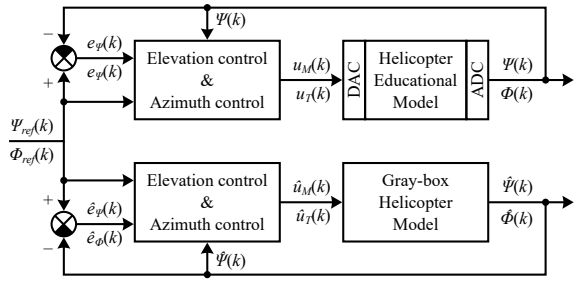

Fig. 12 The control structure for validation of the Helicopter educational model.

The results of the gray-box model validation are shown in Fig. 13, where lower indexes *ref*, *exp* and *sim* denote reference signal, output of the real system and output of the gray-box model respectively. The designed control algorithm is able to stabilize the real system. The elevation subsystem of the real system reacts similarly when compared to the gray-box model. The slight sway at 113 [s] caused by the control algorithm is noticeable in both outputs. When comparing the inputs of the azimuth subsystem, there is a noticeable deviation at the start of the experiment, which is caused by the cross-coupling between the elevation and azimuth subsystems. The initial control input applied to the real system is delayed by approximately 5 [s] to allow the serial interface to be initialized in the Simulink environment. The experimental results show the dependence of the main rotor voltage u_M on the elevation angle Ψ, which has an increasing character if $\Psi < 0$ and a decreasing character if $\Psi > 0$. This effect is caused by the change in amplitude of the normal force by the deviation in the elevation angle Ψ. The dependence of the tail rotor input voltage u_T on the elevation angle Ψ is negligible. The measured data confirms the model of the azimuth subsystem, as the tail rotor input voltage u_T in the steady state is independent of the azimuth angle Φ. The oscillations at the end of the experiment are present in both the elevation Ψ and azimuth Φ angles due to the interactions between the elevation and azimuth subsystems. These oscillations cannot be caused by the control algorithm alone, as its design ignores interactions between subsystems completely. Overall, the results suggest the gray-box model with identified parameters is a suitable approximation of the real system and can be considered as the digital twin.

In this case study, the proposed methodology for the identification of nonlinear dynamic systems is verified on a helicopter educational model. The mathematical model of the helicopter educational model is derived using the physics laws. The model of both rotor subsystems is substituted with a black-box model to improve its accuracy. In total, nine experiments are designed to capture the dynamics of the real system, the data from which is used to estimate the model parameters. The gray-box model is validated in the control structure with the polynomial control algorithm and instantaneous linearization. The validation is done by comparing the gray-box model output $\Psi_{sim}(t)$ with the output of the real system $\Psi_{exp}(t)$. The proposed control algorithm is modified with the aim of its effective deployment on a microcontroller.

4. CONCLUSIONS

The methodology for modeling and identification of nonlinear dynamic systems is proposed in this article, which unifies methods of analytical and experimental identification into a uniform methodology. The proposed methodology is verified within the case study of the identification of the helicopter educational model with modified communication interface. The contribution of the article in this case study is in the design of an extended model of the rotors, as the proposed model captures the dynamic properties of each rotor better compared to the model presented in the educational manual. The design of nine specialized experiments is presented that are mandatory for the estimation of the mathematical model parameters. The data collection required additional sensors (load cell and photogate) to obtain state data for the parameter estimation of the main and auxiliary rotor models. During the parameter estimation of the mathematical model, a unique combination of nonlinear methods is used to estimate the un-

known parameters, thereby reducing the overall computational complexity. The model validation relies on the indirect model validation method, where a polynomial control algorithm with instantaneous linearization is designed in several operational points. The final control algorithm implementation in the STM32 microcontroller required the proposed controller parameter approximation using polynomials. Such implementation reduces the overall computational complexity and allows a short sampling period. The approximation model of the helicopter educational model presented in this case study represents a platform for the verification of advanced control algorithms and state estimation algorithms. Similarly, it presents the digital twin of the real system, which can be used as a synthetic data generator for the training of intelligent models based on neural networks.

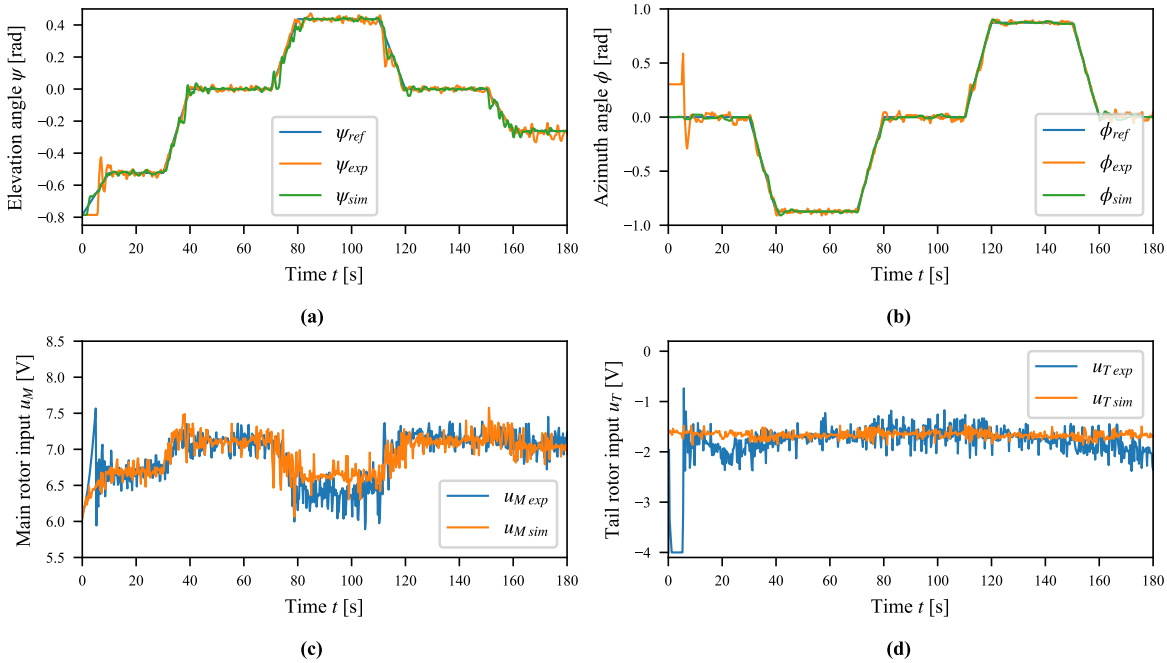

Fig. 13 Gray-box model validation - Helicopter educational model; **(a)** elevation angle Ψ; **(b)** azimuth angle Φ; **(c)** main rotor input u_M; **(d)** tail rotor input u_T.

ACKNOWLEDGEMENT

This work was supported by the Slovak Research and Development Agency under the contract No. APVV-19-0590.

REFERENCES

[1] MAYA-RODRIGUEZ, M. C. - LÓPEZ-PACHECO, M. A. - LOZANO-HERNÁNDEZ, Y. - SÁNCHEZ-MEZA, V. G. - CANTERA-CANTERA, L. A. - TOLENTINO-ESLAVA, R.: Integration of CNN in a Dynamic Model-Based Controller for Control of a 2DOF Helicopter With Tail Rotor Perturbations. In: IEEE Access, 2022, vol. 10. ISSN 2169-3536.

[2] VELAGIC, J. - OSMIC, N.: Fuzzy-Genetic Identification and Control Stuctures for Nonlinear Helicopter Model. In: Intelligent Automation & Soft Computing, 2013, vol. 19, iss. 1, pp. 51-68. ISSN 2326-005X.

[3] CAMACHO, K. M. - BURGOS, J. A. - COMBITA, L. F.: Construction and Modeling of a Two-Degree-of-Freedom Helicopter. In: 2012 Brazilian Robotics Symposium and Latin American Robotics Symposium, 2012, pp. 150-155. ISBN 978-0-7695-4906-4.

[4] Humusoft s.r.o.: CE 150 Helicopter - Educational Manual, 2012.

[5] LEGAT, U. - GAJŠEK, R. - GAŠPERIN, M.: Simulation and Control of Helicopter Pilot Plant. Online: <https://www.academia.edu/12871372/Simulation_and_control_of_a_helicopter_pilot_plant>. Cited on: 2024-07-15.

[6] SALIHBEGOVIC, A. - SOKIC, E. - OSMIC, N. - HEBIBOVIC, M.: High performance disturbance observer based control of the nonlinear 2DOF helicopter system. In: 2013 XXIV International Conference on Information, Communication and Automation Technologies (ICAT), 2013, pp. 1-7. ISBN 978-1-4799-0431-0.

[7] KARER, G. - ZUPANČIČ, B.: Modelling and identification of a laboratory helicopter. In Proceedings of the 5th MATHMOD Conference, 2006, vol. 2, pp. 1-9. ISBN 978-3-901608-29-2.

[8] VELAGIC, J. - OSMIC, N.: Identification and control of 2DOF nonlinear helicopter model using intelligent methods. In: 2010 IEEE International Conference on Systems, Man and Cybernetics, 2010, pp. 2267-2275. ISBN 978-1-4244-6588-0.

[9] NAZARZEHI, V. - FATEHI, A.: Identification of Linear Models for a Laboratory Helicopter. In: 2009 Second International Conference on Computer and Electrical Engineering, 2009, vol. 2, pp. 293-297. ISBN 978-1-4244-5365-8.

[10] AZARMI, R. - TAVAKOLI-KAKHKI, M. - SEDIGH, A. K. - FATEHI, A.: Analytical design of fractional order PID controllers based on the fractional set-point weighted structure: Case study in twin rotor helicopter. In: Mechatronics, 2015, vol. 31, pp. 222-233. ISSN 0957-4158.

[11] OZANA, S. - VOJCINAK, P. - PIES, M. - HAJOVSKY, R.: Control Design of Mixed Sensitivity Problem for Educational Model of Helicopter. In: Advances in Electrical and Electronic Engineering, 2014, vol. 12, no. 5, pp. 488-500. ISSN 1804-3119.

[12] RATHOD, K. - J, M. S.: Robust Control of 2-DoF Helicopter System in Presence of Unmatched Disturbances & Actuator Faults. In: 2022 2nd International Conference on Intelligent Technologies (CONIT), 2022, pp. 1-7. ISBN 978-1-6654-8407-7.

[13] KAFI, M. R. - CHAOUI, H. - MIAH, S. - DEBILOU, A.: Local model networks based mixed-sensitivity H-infinity control of CE-150 helicopters. In: Control Theory and Technology, 2017, vol. 15, no. 1, pp. 34-44. ISSN 2198-0942.

[14] DUTKA, A. S. - ORDYS, A. W. - GRIMBLE, M. J.: Non-linear predictive control of 2 DOF helicopter model. In: 42nd IEEE International Conference on Decision and Control, 2003, vol. 4, pp. 3954-3959. ISSN 0191-2216.

[15] YOUNIS, M. H. - QURAISHI, R.: Adaptive fuzzy control for twin rotor helicopter stabilization. In: 2019 Second International Conference on Latest trends in Electrical Engineering and Computing Technologies (INTELLECT), 2019, pp. 1-5. ISBN 978-1-7281-2435-3.

[16] ZHAO, Z. - HE, W. - MU, C. - ZOU, T. - HONG, K. S. - LI, H. X.: Reinforcement Learning Control for a 2-DOF Helicopter With State Constraints: Theory and Experiments. In: IEEE Transactions on Automation Science and Engineering. 2024, vol. 21, iss. 1, pp. 157-167. ISSN 1558-3783.

[17] DOLINSKÝ, K. – JADLOVSKÁ, A.: Application of Results of Experimental Identification in Control of Laboratory Helicopter Model. In: Advances in Electrical and Electronic Engineering, 2011, vol. 9., iss. 4, pp. 157-166. ISSN 1804-3119.

[18] JADLOVSKÁ, A. – LONŠČÁK, R.: Design and experimental verification of optimal control algorithm for educational model of mechanical system (In Slovak). In: Electroscope, 2008, no I. ISSN 1802-4564.

[19] JAJČIŠIN, Š. - JADLOVSKÁ, A.: Design of predictive control algorithms using the nonlinear models of physical systems (In Slovak). Elfa s.r.o., Košice, Slovakia, 2013, ISBN 978-80-8086-229-9.

[20] LJUNG, L.: System Identification: Theory for the User. Prentice Hall PTR, Hoboken, USA, 1999, ISBN 0-13-656695-2.

[21] NELLES, O.: Nonlinear System Identification: From Classical Approaches to Neural Networks, Fuzzy Models, and Gaussian Processes. Springer International Publishing, Cham, Switzerland, 2020, ISBN 978-3-030-47439-3.

[22] LJUNG, L. - GLAD, T. - HANSSON, A.: Modeling and Identification of Dynamic Systems. Studentlitteratur, Lund, Sweden, 2021, ISBN 91-44-15345-7.

[23] TAKÁCS, G. - VACHÁLEK, J. - ILKIV, B. R.: System identification. STU, Bratislava, Slovakia, 2014. ISBN 978-80-227-4288-7.

[24] NASA - Glenn Research Center: Thrust Equation [cit. 2024-06-28]. URL: <https://www1.grc.nasa.gov/beginners-guide-to-aeronautics/thrust-force/>.

[25] TKÁČIK, T. - TKÁČIK, M. - JADLOVSKÁ, S. - JADLOVSKÝ, J.: Design of Aerodynamic Ball Levitation Laboratory Plant. In: Processes. 2021, vol. 9, iss. 11, pp. 1-19. ISSN 2227-9717.

Received December 12, 2022, accepted February 24, 2023

BIOGRAPHIES

Tomáš Tkáčik (1998) has graduated (MSc) with honors at 2021 at the DCAI of the FEEI at TUKE. After graduation, he has become a PhD. student at the same department. His research is focused on classical and intelligent methods for nonlinear dynamic system identification of physics systems and model validation to design optimal identification methodology for systems at the CMCT&II and CERN.

Anna Jadlovská was born in 1960. She received her MSc. degree in the field of TC at the Faculty of Electrical Engineering of the TUKE in 1984. She defended her PhD thesis in the domain of Automatization and Control in 2001 at the same University; her thesis title was “Modelling and Control of Non-linear Processes Using Neural Networks”. Since 1993 she worked at the DCAI FEEI TUKE as a Associate Assistant and since 2004 she has been working as an Associate Professor. Her main research activities include the problems of adaptive and optimal control – in particular predictive control with constraints for non-linear processes using neural networks and methods of artificial intelligence (Intelligent Control Design). She is the author of scientific articles and contributions to various journals and international conference proceedings, as well as being the co-author of some monographs